Development of High Frequency Interdigital Transducers for NDT of Thin Films

Tahar Kadi, Marc Duquennoy, Mohammadi Ouaftouh, Nikolay Smagin, Frédéric Jenot

Development of High Frequency Interdigital Transducers for NDT of Thin Films

Tahar Kadi, Marc Duquennoy, Mohammadi Ouaftouh, Nikolay Smagin, Frédéric Jenot

Univ. Polytechnique Hauts-de-France, CNRS, Univ. Lille, Yncréa, Centrale Lille, UMR 8520 - IEMN, DOAE, F-59313 Valenciennes, France
Correspondence marc.duquennoy@uphf.fr

ABSTRACT

Various engineering systems components suffer destructive effects on their surfaces, like wear, fatigue, or corrosion during their operation. Protecting the surface by hardening treatments or applying coatings is a widespread way to extend their life and improve the product quality. Important properties of surface films and coatings are thickness, adhesion to the substrate, hardness, elastic modulus, thermal conductivity, electrical conductivity and others. The dispersion of surface acoustic waves (SAW) can be used to determine mechanical and geometrical film parameters such as Young's modulus and film thickness. Especially, Young's modulus is an important parameter for nondestructive characterization of film materials. In order to determine the film properties, the dispersion curve $v(f)$ is measured and fitted by a theoretical curve. The SAW penetration depth is of the order on a wavelength, and thus it can be varied by varying the SAW frequency. In order to generate high frequency surface waves ($f > 200$ MHz), we have developed chirped-type broadband (20–240 MHz) interdigital transducers. These transducers have been optimized, characterized and used in several NDT applications.

1. INTRODUCTION

Functional coatings and thin films deposited on substrates are highly sought-after in numerous applications. Such additional layers may be applied to improve the durability of structures, including wear and fatigue resistance, or to obtain specific physical or electronic properties. The characterization of these coatings and layers consists in determining their mechanical and geometrical properties (thickness, elastic constants, adhesion, residual stress, etc.); it allows the state of separate structural elements to be monitored and ensures optimum operation when in use. Among others, various ultrasonic methods have proven to be efficient for non-destructive testing (NDT) of layered structures [1]. Among the various types of ultrasonic waves that propagate near the surface boundary, Rayleigh surface acoustic waves (SAW) are particularly interesting as their energy is concentrated within a thin layer under the surface about one wavelength thick. In the case of broadband Rayleigh wave propagation, different spectral components have non-equal penetration depths in the layer and in the substrate leading to the dispersion phenomena [2-4].

For example, a wave with a frequency high enough to propagate entirely within the surface layer is affected only by the characteristics of the layer. Inversely, a much lower frequency wave is mostly sensitive to the substrate properties; the effect is illustrated in figure 1. Frequency-dependent Rayleigh SAW propagation along thin coatings can be exploited to characterize the latter [5-7]. Indeed, in order to obtain a high precision of inversion procedure used to determine the dimensional or mechanical surface characteristics, it is necessary to obtain a sufficiently considerable velocity variation over the selected frequency range [8].

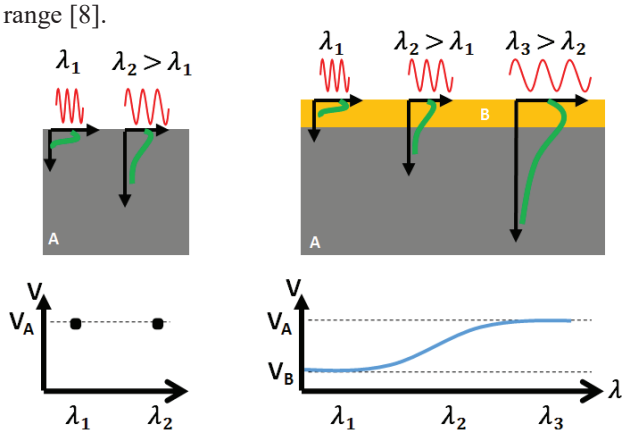

Figure 1. Illustration of the decay of Rayleigh waves penetration depth with frequency and dispersion phenomena. V_A and V_B are the velocities of the Rayleigh waves in the substrate and in the thin Gold layer, respectively.

Nanoscale layer thicknesses correspond to SAW wavelengths in the gigahertz frequency range. However, it has been demonstrated that even if the wavelengths are greater than a micrometer and, therefore, the thicknesses of the coatings, they remain sensitive to the characteristics of the latter [9-10]. By generating SAW over a very high frequency range $(20 - 240\ \text{MHz})$ rather than an ultra-high frequency range $(200 - 2400\ \text{MHz})$, it is possible to envisage wave propagation along a coating surface of several millimeters or tens of millimeters, which is a substantial advantage in terms of characterization [11-13]. Several techniques have been used to generate Rayleigh-type surface waves, including laser-ultrasound [14-15], wedges [16], immerged transducers line-focus acoustic transducers [17] or interdigital transducers (IDTs) [11-13]. The latter allows broadband SAW generation on a piezoelectric substrate in an easily controllable way using

a chirped configuration [18]. Since IDTs are extraneous relatively to the structure-under-test in NDT applications, it is necessary to provide sustainable acoustical contact. This issue is sometimes circumvented by integrating IDT electrodes and the piezoelectric substrate directly into the structure [19-20] yelding unavoidable limitations with configurations of the test samples. Thanks to the proposed solution (external transducer), it is possible to characterize the structures, as with conventional NDT methods, without altering or modifying the tested structures (thin layer structures).

Our original approach to resolve the mentioned issue consists in bringing a SAW-IDT, on which the fingers are deposited, in contact with the sample. In the area where the IDT piezoelectric substrate and the sample are touching, the wave is transmitted and propagates in the sample, figure 2.

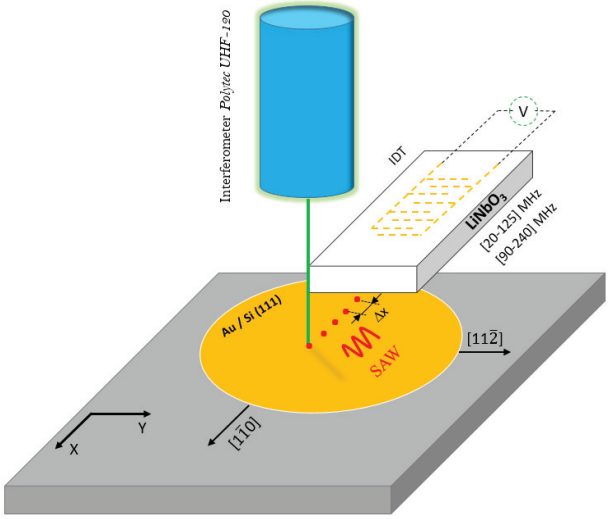

Figure 2. Schematic representation of the experimental setup.

Previously, we successfully measured the velocity dispersion on thin layer samples using a series of mono-frequency contact IDTs [11]. In this work, we report measurements using a single wideband IDT which offers a substantial gain in measurement time and precision [21].

We recently demonstrated that a chirped IDT could be excited with a temporal chirp (temporal-spatial chirp technique), which makes it possible to achieve higher SAW amplitudes while operating at a much lower voltage than the breakdown threshold [22]. In this work, we characterized thin gold layers (approximately 300 nm thick and 180 nm) deposited by thermal evaporation on a silicon (111) substrate. In order to generate SAW with only two transducers and to limit manipulation, wideband IDTs with bandwidths 20-125 MHz and 90- 240 MHz were realized. Dispersion curves were obtained using the Slant Stack method [23]. The inversion procedure was then applied in order to determine the sample's properties (E,ν).

2. ESTIMATION OF PHASE VELOCITY

In this study, the thin layers were characterized by exploiting SAW dispersion. The measurement procedure involved several steps. First, SAWs were generated using an IDT transducer and transmitted to the test sample. The waves were then detected using an interferometer sensitive to the normal displacements generated by these waves. In the experiment, SAW's propagate along the Si(111)[1$\bar{1}$0] and Si(111)[11$\bar{2}$] directions. In order to obtain dispersion curves, a B-scan along the X direction (Fig. 2) was made using the laser Doppler vibrometer.

Several methods exist to determine the phase velocity dispersion from the normal displacements obtained by means of an interferometer. In our case, we chose the Slant Stack transform. This method is fast and efficient and allows the velocities to be estimated with high precision [24]. This method is known as τ-p transform. The signal processing makes it possible to determine the phase velocity as a function of frequency. The method is detailed in particular for the case of Rayleigh waves in [25-26]. In terms of precision, the results obtained with this method were as performant as other methods (2DFFT, wavelet). In addition, the dispersion curves could be plotted directly [25].

In the following section, we will present the type of IDT transducer used for generating SAW and the interferometer used to measure normal displacements.

2.1 Interdigital transducers for generating surface acoustic waves

A SAW-IDT consists of two overlapping metal comb-shaped electrodes with interdigitated fingers and a coverage length W_a. The electrodes are deposited on a piezoelectric substrate. Consequently, when a voltage U is applied between the two electrodes, there is an accumulation of charges of which the signs alternate from one finger to the other thus creating an electric field between each pair of electrodes. The combination of the piezoelectric effect of the substrate and the electric field generates expansions and compressions in the material thus creating movement. This movement gives rise to surface waves perpendicular to the electrode fingers. In this study, the piezoelectric substrate was of lithium niobate (128° YX), as this material has a very high electromechanical coupling coefficient ($K^2 = 5.3\%$).

For the IDT excitation adapted with the dual temporal-spatial method, a linear frequency swept signal ranging from 20 to 125 MHz and from 90 to 240 MHz with a duration of 1 µs is needed. Thus, the time-frequency product is equal to approximately 100. This is practical for applications in terms of IDT size, total emitted energy, and Fresnel ripples level.

2.2 Principle of interferometer imaging device

In order to characterize the SAW displacement field generated by this broadband IDT, we used a scanning laser Doppler vibrometer, LDV (PolytecUHF-120). This heterodyne-type apparatus allows the out-of-plane vibrational component to be measured in the frequency range from DC to 1.2 GHz. The SAW displacement sensitivity threshold is defined as 30 fm·√(f (Hz)), where "fm" stands for femtometers and f is the frequency in

Hertz. For f = 240 MHz and 64 averaged sweeps used in the present work, this gives a displacement noise level of approximately 30 pm. The spatial scanning resolution isdefined by the motorized stages and equals to 300 nm.
In the experimental setup (Fig. 2),the thin layer of gold deposited on a 3-inch silicon (111) wafer was fixed on a motorized XY stage. Sensing was performed using a Polytec UHF-120 laser and video scanning head. The signal received by the scanning head's photodiode was digitized using a LeCroy 725Zi-A oscilloscope and transferred to a computer (PC) for digital IQ demodulation. The chirped signals were generated using a Tektronix 7051 arbitrary waveform generator. Furthermore, the signal voltage was increased to 20 V using an Amplifier Research 50W1000A power amplifier (1–1000 MHz frequency band, 50 W).

3. INVERSE PROBLEMS AND EXPERIMENTAL CHARACTERIZATION OF THE LAYER–ON-SUBSTRATE STRUCTURE

Since the dispersion curves are directly related to the elastic properties and the densities of the two materials, as well as to the thickness of the layer, they can be calculated theoretically [27]. In our case, the densities of the gold layer and the silicon substrate were known accurately [28] and the estimation of the layer thickness and Young's modulus from the measured phase velocities, consisted in solving the inverse problem. An inverse method was used to determine the thickness and Young's modulus, which provides theoretical propagation velocities that are as close as possible to those measured experimentally. The selected optimization method thus allows obtaining the closest fit of theoretical velocities to the measured velocities.
The approximate values of the elastic coefficients of gold from the bibliographic data provided an initial estimate of the phase velocities (Table 1). For the substrate, theoretical SAW velocities were calculated using the elastic constants C_{11}=165.7 GPa, C_{12}=63.9 GPa and C_{44}= 79.56 GPa, E = 78 GPa and the density ρ= 2330 kg/m^3. A minimization routine was then executed to find the thickness of the layer. A least squares minimization was carried out. The processing algorithm then sought to maximize the value of the regression coefficient R^2 [11].

Parameter	Gold layer
Density ρ (g/cm3)	19.3
Longitudinal wave velocity (m/s)	3212
Shear wave velocity (m/s)	1193
Rayleigh wave velocity (m/s)	1127

Table 1. Characteristics of the Gold layer considered as isotropic.

For example, the inverse method procedure, we defined thicknesses between 130 and 230 nm with a step of 0.001 nm. The dispersion curve was plotted using different thickness values. Finally, the estimated layer thickness was 176nm (figure 3).

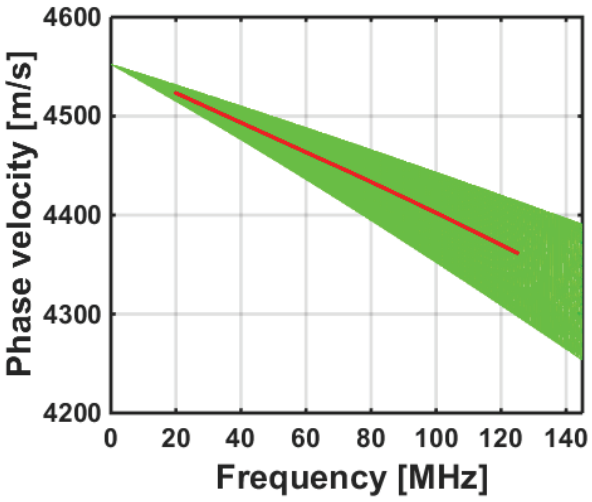

Figure 3. Resulting measured dispersion curve, and its fitted curve from the theoretical model. Experimental dispersion curve (red line) and in green lines the theoretical dispersion curves.

The thicknesses determined using our inversion procedure were compared with the measurements obtained using a KLA-Tencor Asic surface profiler. Several non-covered regions were intentionally left near the boundaries of the sample. These "steps" formed between the Gold-covered and non-covered regions permitted profilometer measurements. In numerous practical cases, such measurements are not possible due to the absence of such features.

3.1 Measurement of the surface acoustic wave velocity on silicon (111) single crystals using IDT-SAW along two crystallographic directions, [1$\bar{1}$0] and [11$\bar{2}$]

Surface acoustic wave (SAW) were excited on the (111) plane of silicon single crystals using an IDT-SAW in the range of [20-125] MHz. For the Si (111) plane the SAW velocities were measured between the [1$\bar{1}$0] direction and the [11$\bar{2}$] direction. The velocity increases from 4548(m/s) along [1$\bar{1}$0] to 4746 (m/s) in the [11$\bar{2}$] direction as shown in figure 4.

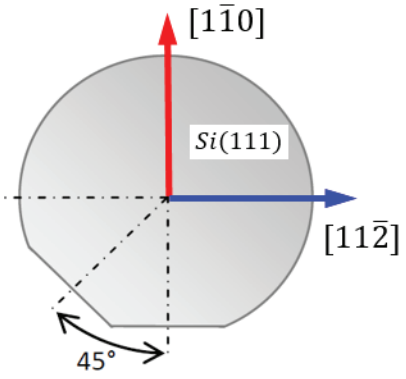

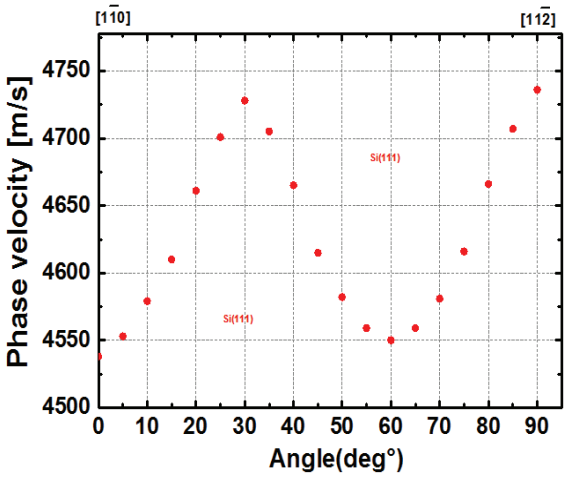

Figure 4. SAW velocities measured on the Si (111) plane.

3.2 Thickness and Young's modulus determination for the thin gold layers

Figure 5 illustrates the modification of chirped SAW due to dispersion. The seven A-scan signals presented in figure 5(a) correspond to the locations equally spaced between the starting and ending points of the B-scan along theSi(111)[1$\bar{1}$0] direction. SAW displacement is of the nanometer order and it is possible to observe that the attenuation is not considerable and by inversion, layer thickness and Young's modulus can be estimated. In other studies, residual stresses could be measured [12-13]. Figure 5(b) shows the resulting dispersion curve calculated from slant-Stack transform in the frequency range of [20-125] MHz.

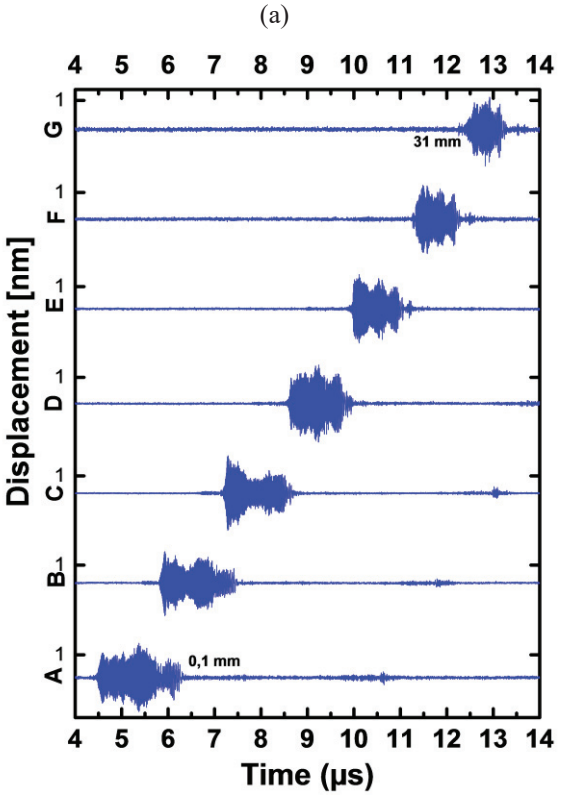

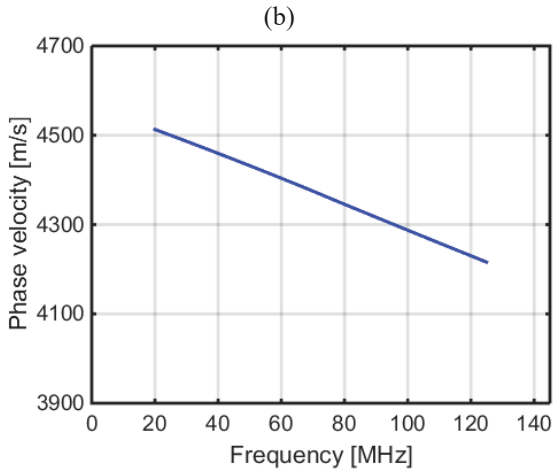

Figure 5. (a) Dispersive Rayleigh wave signals measured after different propagation distances; (b) Resulting measured dispersion curve in the frequency range of [20-125] MHz for the 300 nm gold layer.

Figure 6 shows the measured dispersion curves of the samples, having different Au thickness (180 nm and 300 nm). As theory and experiment predicts, all the curves approach the substrate Rayleigh wave velocity at low frequency, V_R= 4548 (m/s) along Si(111)[1$\bar{1}$0]direction and V_R= 4743 (m/s) along Si(111)[11$\bar{2}$]direction. In order to deduce the mechanical properties and dimensional parameters of the gold layers, an iterative inversion procedure is used to find the best combination of the properties of both the substrate and the thin gold layer. The combination of these parameters allows plotting the best theoretical curve [9] that fits the one obtained experimentally. Figure 6 also represents the best fit of the experimental curves (continuous line) with the theoretical curve (dotted line). The fit is obtained in the frequency range 0–300 MHz. The curve was fitted with the inversion calculation until the intercept with the ordinate axis corresponds to the velocity of the Rayleigh wave of the substrate, $v_{R_{(Si\ (111)[1\bar{1}0])}}$= 4549 m/s and $v_{R_{(Si(111)\ [11\bar{2}])}}$= 4746 m/s. The fit is good within the majority of points

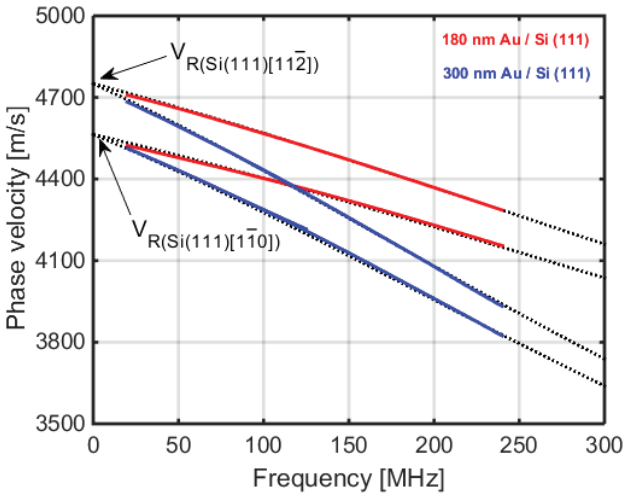

Figure 6. Resulting measured dispersion curve (solid line), and its fitted curve from the theoretical model (dotted line).

Tables 3 and 4 contains the values of the fitted parameters of the samples in the $[1\bar{1}0]$ and $[11\bar{2}]$ direction, respectively.

Parameter	180 nm Au	300 nm Au	Substrate Si (111) $[1\bar{1}0]$
Wafer size (inch)	-	-	3
Thickness (nm)	176	298	2.10^6
Young's modulus (GPa)	76.3	79.6	144.3
Poisson's ratio	0.44	0.43	0.265

Table 3. Parameters of the Gold layers / Si $(111)[1\bar{1}0]$ substrate test sample.

Parameter	180 nm Au	300 nm Au	Substrate Si (111) $[11\bar{2}]$
Wafer size (inch)	-	-	3
Thickness (nm)	182	301	2.10^6
Young's modulus (GPa)	76.5	79.3	157
Poisson's ratio	0.44	0.43	0.27

Table 4. Parameters of the Gold layers / Si $(111)[11\bar{2}]$ substrate test sample.

In order to confirm these results, the thickness of the gold layer for each sample was measured using a high-precision profilometer, the results are shown in Figure 7. The profilometric measurement is based on a local thickness measurement (made on the edges of the deposit), while the ultrasonic method (dispersion of surface acoustic waves) corresponds to averaged measurements made on a region of the sample (here, located in the center of the deposit). The agreement between the directly measured and fitted Au thicknesses seems to be quite good.

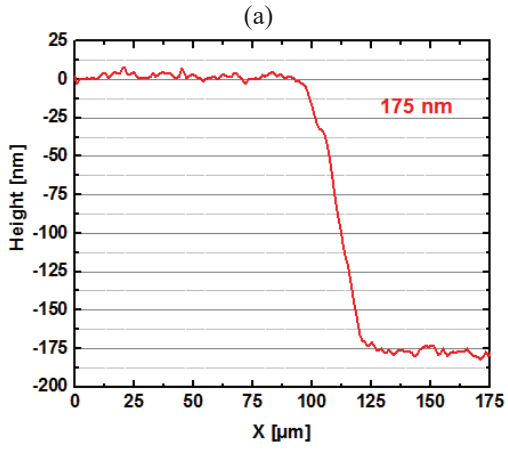

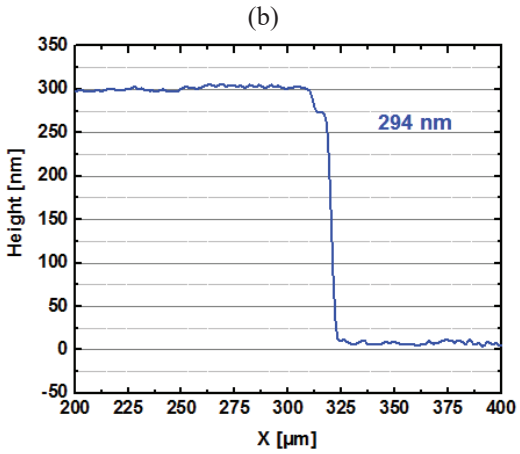

Figure 7. Profilometric evaluation of the thickness of the gold layer for the samples 180 nm Au (a) 300 nm Au (b).

4. DISCUSSION

The results presented above clearly highlight the great interest of a chirp wideband IDTs for NDT of thin layers. Using a wideband Rayleigh source with a 20–125 MHz and 90-240 MHz frequency range, a variation in SAW velocity in the order of 750 m/s (Si(111)$[1\bar{1}0]$)and 420 m/s (Si(111)$[11\bar{2}]$) can be obtained for the 300 nm and 180 nm thick layer, respectively. Thus, using only two IDTs and a single LDV longitudinal scanning, it is possible to measure an entire dispersion curve. This results in a substantial gain in measurement time compared with covering the required frequency band with sets of single-frequency IDTs [7].

Comparing the results obtained for the measurements along the direction Si(111)$[11\bar{2}]$ with those obtained along the direction Si(111)$[1\bar{1}0]$ and taking in consideration the anisotropy of the substrate a very good correlation between thicknesses and Young's moduli can be observed for the two samples. This correlation shows that the inversion method is sensitive to the mechanical properties of the substrate in addition to the properties of the gold thin films. The small difference in terms of estimated thicknesses along the $[11\bar{2}]$ direction and along $[1\bar{1}0]$ can perhaps be explained by the non-uniformity of the thickness of the thin film over the entire surface of the wafer 3 inches. As the direction are different, so are the areas inspected.

The results in terms of thickness obtained by profilometry show a good correlation with those estimated with the inversion method. It is important to specify that thickness measurements using a profilometer are performed in a localized manner on a step (step height between the uncoated substrate and the substrate coated with the gold thin film), while the ultrasonic method (dispersion of surface waves) corresponds to measurements carried out on a region of the sample.

The mechanical properties of the silicon substrate (111) are direction-dependent due to anisotropy. The developed ultrasonic method is sensitive to this effect of anisotropy because part of the energy of the surface acoustic wave

propagates in the substrate and the inversion procedure allows estimating the mechanical properties (E,ν) of the substrate in the crystallographic directions $[1\bar{1}0]$ and $[11\bar{2}]$which are respectively, $(E = 144.3\ \text{GPa},\ \nu = 0.265)$ and $(E = 157\ \text{GPa},\ \nu = 0.27)$.

The Young's modulus values of gold thin films estimated by the ultrasonic method are slightly different from the Young's modulus value of bulk gold, which is 79 GPa. Several research works show that it is common to have a different Young's modulus between the thin film and bulk material. The difference in Young's modulus for the gold thin films in samples (300 nm and 180 nm) could be explained by the crystallographic orientation of the grains (crystallites) that make up the gold thin films, as well as the evolution of grain size as the thickness of the thin film increases [29,30]. For a thin gold layer, the grain size evolves with the layer thickness. A 100 nm thin layer consists of grains with a size of 40 nm, 60 nm for a 300 nm thick layer and 80 nm for a 500 nm thickness [31].

5. CONCLUSION

This study presents an ultrasonic method for characterizing thin films based on the dispersion of surface acoustic waves. The measuring principle, which consists in generating SAW on the layer-on-substrate structure to be characterized, was presented. It was then specified that the SAWs should be generated over a frequency range high enough for the waves to be sensitive to thin deposits but still between 20 MHz and 240 MHz where the attenuation was reasonable and measurements could thus be made over 20 mm of SAW propagation length. Furthermore, thanks to the phenomenon of dispersion, we obtain significant variations in phase velocity, which then guarantees a precise inversion. It was shown that wide-band transducers capable of efficiently generating SAWs over the entire frequency range between 20 MHz and 240 MHz were required. Finally, two samples on which gold layers of 300 nm and 180 nm thick had been deposited were characterized. The thicknesses, as well as the elastic parameters of the gold layers and the silicon substrate, could be determined from the inversions performed on the experimental dispersion curves.

ACKNOWLEDGMENTS

This work was supported by ELSAT 2020 project. The ELSAT 2020 project was co-financed by the European Union through the European Regional Development Fund, the French government, and the Hauts-de-France Regional Council. This work was also supported by the French RENATECH network.

6. REFERENCES

[1] D. O. Thompson and D. E. Chimenti, *Review of Progress in Quantitative Nondestructive Evaluation*. New York, NY: Springer, 2013.

[2] G. W. Farnell and E. L. Adler, “Elastic Wave Propagation in Thin Layers,” in *Physical Acoustics*, vol. 9, Elsevier, 1972, pp. 35–127.

[3] T. W. Murray, S. Krishnaswamy, and J. D. Achenbach, “Laser generation of ultrasound in films and coatings,” *Applied Physics Letters*, vol. 74, no. 23, pp. 3561–3563, Jun. 1999.

[4] A. Ben-Menahem and S. J. Singh, “Surface-Wave Amplitude Theory,” in *Seismic Waves and Sources*, New York, NY: Springer New York, 1981, pp. 257–336.

[5] Z. Liu, B. Lin, X. Liang, and A. Du, “Time-frequency analysis of laser-excited surface acoustic waves based on synchrosqueezing transform,” *Ultrasonics*, vol. 106, p. 106147, Aug. 2020.

[6] X. Xiao, H. Qi, Y. Tao, and T. Kikkawa, “Study on the interfacial adhesion property of low-k thin film by the surface acoustic waves with cohesive zone model,” *Applied Surface Science*, vol. 388, pp. 448–454, Dec. 2016.

[7] D. Fall, M. Duquennoy, M. Ouaftouh, N. Smagin, B. Piwakowski, and F. Jenot, “Non-destructive characterization of surfaces and thin coatings using a large-bandwidth interdigital transducer,” *Review of Scientific Instruments*, vol. 89, no. 12, p. 124901, Dec. 2018.

[8] P. Rajagopal, K. Balasubramaniam, S. Maddu, and C. V. Krishnamurthy, “A new approach to inversion of surface wave dispersion relation for determination of depth distribution of non-uniform stresses in elastic materials,” *International Journal of Solids and Structures*, vol. 42, no. 3–4, pp. 789–803, Feb. 2005.

[9] C. K. Campbell, Surface acoustic wave devices for mobile and wireless communications. San Diego, Calif.: Academic Press, 1998.

[10] D. Royer and E. Dieulesaint, *Elastic waves in solids. I, I,*. Berlin; London: Springer, 2011.

[11] J. Deboucq, M. Duquennoy, M. Ouaftouh, F. Jenot, J. Carlier, and M. Ourak, “Development of interdigital transducer sensors for non-destructive characterization of thin films using high frequency Rayleigh waves,” *Review of Scientific Instruments*, vol. 82, no. 6, p. 064905, Jun. 2011.

[12] M. Duquennoy, M. Ouaftouh, J. Deboucq, J.-E. Lefebvre, F. Jenot, and M. Ourak, “Influence of a superficial field of residual stress on the propagation of surface waves—Applied to the estimation of the depth of the superficial stressed zone,” *Applied*

Physics Letters, vol. 101, no. 23, p. 234104, Dec. 2012.

[13] M. Duquennoy, M. Ouaftouh, J. Deboucq, J.-E. Lefebvre, F. Jenot, and M. Ourak, "Characterization of micrometric and superficial residual stresses using high frequency surface acoustic waves generated by interdigital transducers," The Journal of the Acoustical Society of America, vol. 134, no. 6, pp. 4360–4371, Dec. 2013.

[14] X. Xiao, T. Kong, H. Y. Qi, and H. Q. Qing, "Nondestructive determination of film thickness with laser-induced surface acoustic waves," Chinese Physics B, vol. 27, no. 9, p. 096802, Sep. 2018.

[15] A. Yin *et al.*, "Texture in steel plates revealed by laser ultrasonic surface acoustic waves velocity dispersion analysis," *Ultrasonics*, vol. 78, pp. 30–39, Jul. 2017.

[16] B. R. Tittmann, L. A. Ahlberg, J. M. Richardson, and R. B. Thompson, "Determination of Physical Property Gradients from Measured Surface Wave Dispersion," *IEEE Transactions on Ultrasonics, Ferroelectrics and Frequency Control*, vol. 34, no. 5, pp. 500–507, Sep. 1987.

[17] F. Lakestani, J.-F. Coste and R.Denis, "Application of ultrasonic Thickness Measurement of Metallic coatings," NDT International 28(1995)3, p. 171 - 178.

[18] E. K. Sittig, "Design and Technology of Piezoelectric Transducers for Frequencies Above 100 MHz," in *Physical Acoustics*, vol. 9, Elsevier, 1972, pp. 221–275.

[19] K. Toda, G. Sugizaki, T. Takenaka, and K. Sakata, "A technique for measuring strain in layered structure media," *Sensors and Actuators A: Physical*, vol. 43, no. 1–3, pp. 213–216, May 1994.

[20] T.-W. Liu, Y.-C. Tsai, Y.-C. Lin, T. Ono, S. Tanaka, and T.-T. Wu, "Design and fabrication of a phononic-crystal-based Love wave resonator in GHz range," *AIP Advances*, vol. 4, no. 12, p. 124201, Dec. 2014.

[21] J. M. Richardson, "Estimation of surface layer structure from Rayleigh wave dispersion: Dense data case," *Journal of Applied Physics*, vol. 48, no. 2, pp. 498–512, Feb. 1977.

[22] D. Fall, M. Duquennoy, M. Ouaftouh, N. Smagin, B. Piwakowski, and F. Jenot, "Generation of broadband surface acoustic waves using a dual temporal-spatial chirp method," *The Journal of the Acoustical Society of America*, vol. 142, no. 1, pp. EL108–EL112, Jul. 2017.

[23] T. Kadi *et al.*, "Dimensional and mechanical characterization of metallic thin films based on the measurement of surface acoustic waves dispersion with Slant Stack transform," *Measurement Science and Technology*, vol. 31, no. 10, p. 105009, Jul. 2020.

[24] G. A. McMechan and M. J. Yedlin, "Analysis of dispersive waves by wave field transformation," *GEOPHYSICS*, vol. 46, no. 6, pp. 869–874, Jun. 1981.

[25] L. Ambrozinski, B. Piwakowski, T. Stepinski, and T. Uhl, "Evaluation of dispersion characteristics of multimodal guided waves using slant stack transform," *NDT & E International*, vol. 68, pp. 88–97, Dec. 2014.

[26] R. Askari and S. H. Hejazi, "Estimation of surface-wave group velocity using slant stack in the generalized S-transform domain," *GEOPHYSICS*, vol. 80, no. 4, pp. EN83–EN92, Jul. 2015.

[27] I. A. Viktorov, *Rayleigh and Lamb waves: physical theory and applications*. New York: Springer Science + Business Media, 2013.

[28] C. C. W. Ruppel, Ed., Advances in surface acoustic wave technology, systems and applications. Vol. 1 Singapore: World Scientific, 2000.

[29] A. J. Kalkman, A. H. Verbruggen, and G. C. A. M. Janssen, "Young's modulus measurements and grain boundary sliding in free-standing thin metal films," *Applied Physics Letters*, vol. 78, no. 18, pp. 2673–2675, Apr. 2001.

[30] D. Faurie *et al.*, "Elastic properties of polycrystalline gold thin films: Simulation and X-ray diffraction experiments," *Surface and Coatings Technology*, vol. 201, no. 7, pp. 4300–4304, Dec. 2006.

[31] C. Birleanu and M. Pustan, "The effect of film thickness on the tribomechanical properties of the chrome-gold thin film," in *2016 Symposium on Design, Test, Integration and Packaging of MEMS/MOEMS (DTIP)*, Budapest, Hungary, May 2016, pp. 1–6.